34th Annual International Conference of the IEEE EMBS
San Diego, California USA, 28 August - 1 September, 2012

A Fast Torsionally Compliant Kinematic Model of Concentric-Tube Robots

R. Xu, *Student Member, IEEE,* and R. V. Patel, *Fellow, IEEE*

Abstract— **Concentric-tube robots have the potential to become an important surgical tool for robot-assisted percutaneous interventions. They can provide dexterous operation in a small constrained environment. The kinematic model of a concentric-tube robot has been well developed in terms of accuracy, but the computational cost places limitations on real-time implementation. In this paper, we propose a new technique that will substantially improve the computational efficiency of evaluating the kinematics of a concentric-tube robot in the context of developing a control strategy without sacrificing the accuracy of the results. In this paper we develop a torsionally compliant kinematic model using global variables. The model is validated by comparing the results obtained by computing the kinematic model corresponding to an experimental setup of a concentric-tube robot to which a force/torque sensor has been mounted at its base with those obtained directly from the experimental setup. The results indicate that it is feasible to compute the kinematics of the concentric-tube robot fast enough to allow the position/force control loop to be implemented at a rate of 1 kHz.**

I. Introduction

The concentric-tube robots are a new type of continuum robots. A concentric-tube robot consists of several pre-curved elastic tubes inserted one inside another. By translating and rotating two consecutive tubes relative to each other, this kind of robot can achieve to fairly complex 3D shapes. The concentric-tube robot is suitable for surgical environments because it can offer more than 5-DOF (degrees of freedom) with dimensions as small as those of a needle (typically less than 3mm in diameter).

In recent years, various kinematic models of concentric-tube robots have been proposed based on different considerations. The model proposed in [1] is simple but has limited application, since it requires that the stiffness of the outer tubes is nearly infinite compared to that of the inner tubes. Torsionally rigid models were developed in [2], with the assumption that the tubes only experience bending. The position and orientation of the robot can be obtained analytically regardless of the ratios of stiffness between tubes, and the inverse kinematics also exists in closed form [3]. The importance of introducing torsion effects into the model was shown experimentally in [4]. A kinematic model that contains the torsion of the straight section of robots was proposed in [4]. Although the solution of this model has to be evaluated numerically, the Jacobian kinematics can be obtained in closed form [5]. A torsionally compliant model that includes the torsion effects of both straight and curved sections presents significant improvement with regard to accuracy [6], [7]. However, this model is computationally very expensive, because it involves solving a set of nonlinear differential equations with two-point boundary conditions. Additional calculations are needed because the solutions do not give the robot's position and orientation directly. Other comprehensive models have also been developed by considering the friction effects in the tubes [8] or external loads [9]. The complexity of these models increases as more mechanical effects are included. Efforts have been made to achieve a trade-off between computational efficiency and numerical accuracy. In [10] a function approximation method was developed to implement a torsionally compliant model in real-time for position control with minimum loss of accuracy. However, the approach requires pre-computation of a large dataset of position and orientation information over the entire workspace. A Fast Jacobian-based inverse kinematic algorithm was presented in [11], and it was shown that the computational time can be reduced to 40 ms for a 3-tube robots.

In this paper, we propose a technique which can significantly decrease the computation time to evaluate a torsionally compliant model in the context of implementing a kinematic control strategy for a concentric-tube robot. This is achieved by improving the model in the following aspects:

- Reformulating the torsionally compliant kinematic model with global variables.
- Measuring all the initial conditions to avoid the two-point boundary problems. These measurements (which are obtained in real-time during the implementation of a kinematic control strategy) provide inputs for computing the model used in kinematic control of the robot.
- Piecewise-linearization of the reformulated model.

It is shown from the experiments that the computation time is reduced to less than 1ms using this technique (see Section III.). At the same time, the accuracy of this model remains almost equivalent to that of the torsionally compliant models proposed in the literature.

This research was supported by a grant from the Natural Sciences and Engineering Research Council (NSERC) of Canada under grants RGPIN-1345 (R.V. Patel), and by infrastructure grants from the Canada Foundation for Innovation awarded to the London Health Sciences Centre (Canadian Surgical Technologies & Advanced Robotics (CSTAR)) and to The University of Western Ontario (UWO) (R.V. Patel). Partial financial support for R. Xu has been provided by a postgraduate scholarship from the Peoples Republic of China.

R. Xu is with CSTAR, Lawson Health Research Institute, 339 Windermere Road, London, ON, Canada and with the Department of Electrical and Computer Engineering, UWO, London, ON, Canada (email: rxu25@uwo.ca). R.V. Patel is with CSTAR, the Department of Electrical and Computer Engineering and the Department of Surgery, UWO (email: rvpatel@uwo.ca).

II. KINEMATIC MODEL

A. Cosserat Rod

Cosserat rod theory is extensively used in modeling and simulation of slender elastic objects. The elastic tubes used in concentric-tube robots are actually a very good example of Cosserat rods in 3-D space. The recent kinematic models of concentric-tube robots, including our work, also follow the notation and formulation from the Cosserat model. Therefore, it is necessary to summarize some relevant background concerning Cosserat rod theory.

Fig.1 shows a flexible rod in the world-frame $\{e_1, e_2, e_3\}$. A body frame $\{ d_1(s), d_2(s), d_3(s) \}$ is attached at an arbitrary cross-section of the rod, where *s* is the arc length along the center line. The position of this cross-section is represented by the vector *r(s)*, and the orientation is defined by the rotation matrix *R(s)* between two frames. When the rod experiences a distributed force *f(s)* and moment *l(s)*, the equations of equilibrium [13] have the following form:

$$\dot{n}(s) + u(s) \times n(s) + f(s) = 0 \tag{1a}$$

$$\dot{m}(s) + u(s) \times m(s) + v(s) \times n(s) + l(s) = 0 \tag{1b}$$

where the vector $u(s) = \begin{bmatrix} u_x(s) & u_y(s) & u_z(s) \end{bmatrix}^T$ includes the bending curvature $(u_x(s), u_y(s))$, and the torsional curvature $u_z(s)$; and $v(s) = \begin{bmatrix} v_x(s) & v_y(s) & v_z(s) \end{bmatrix}^T$ denotes the shear strain $(v_x(s), v_y(s))$ and elongation $v_z(s)$. Both of these vectors are local variables in body frames.

In Cosserat rod theory, curvatures are interpreted as angular rates of change when the body frame slides along the center line. So they have the same expressions as the angular velocity in rigid-body motion:

$$[u(s)] = R^T(s)\dot{R}(s) \tag{2}$$

where $[u(s)]$ is the skew-symmetric matrix corresponding to the vector $u(s)$. Similarly, the shear strain and elongation are analogous to displacements in rigid-body motion and formulated as:

$$v(s) = R^T(s)\dot{r}(s) \tag{3}$$

But in our application, these phenomena can be ignored which results in $v(s) = [0, 0, 1]$.

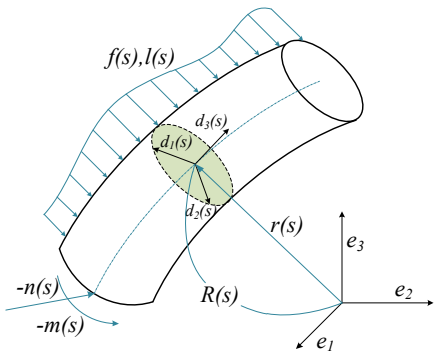

Figure 1. Cosserat rod

B. Torsionally Compliant Model

Torsionally compliant models show great improvements on accuracy, compared to previous models. The equations from this model also play an important role in our method, so a brief description is exhibited here.

For concentric-tube robots, the following assumptions are made for modeling: 1) At any point along the robot, all the assembled tubes conform to the same curvature; 2) without an external force or moment, the net moment at every cross section of the robot is zero; 3) the bending moment generated by a single tube obeys a linear constitutive equation (arc length s will be omitted for compact expressions):

$$m_i = K_i(u_i - \hat{u}_i) \tag{4}$$

in which $\hat{u}_i$ and u_i are the curvatures of the *ith* tube before and after the conformation, respectively. In the rest of this paper, the subscript *i* refers to the *ith* tube. K_i is the stiffness matrix ($K_i = diag\begin{bmatrix} k_{ix} & k_{iy} & k_{iz} \end{bmatrix}$). Based on these assumptions, the bending curvature of the combined tubes can be formulated as:

$$\begin{bmatrix} u_{ix} \\ u_{iy} \end{bmatrix} = \left(\left(\sum_{j=1}^{n} K_j \right)^{-1} R_z^T(\alpha_i) \left(\sum_{j=1}^{n} R_z^T(\alpha_i) K_j \begin{bmatrix} \hat{u}_{jx} \\ \hat{u}_{jy} \end{bmatrix} \right) \right) \tag{5}$$

where $\alpha_i(s)$ represents the angle difference between the body-frames of tube *i* and the *1st*, and $R(\alpha_i(s))$ represents the rotation matrix between those two, as shown in Fig. 2.

The formulation of the torsional curvature is achieved by using equations of equilibrium (1b) from Cosserat rod theory and the constitutive equation (4):

$$\dot{u}_{iz} = \left(\frac{k_{ix}}{k_{iz}} \right) (u_{ix}\hat{u}_{iy} - u_{iy}\hat{u}_{ix}) \tag{6}$$

By definition of $\alpha_i(s)$ and u_{iz}, we can also conclude:

$$\dot{\alpha}_i = u_{iz} - u_{1z} \tag{7}$$

Equations (5), (6) and (7) comprise the torsionally compliant model in [6], with boundary conditions $\alpha_i(0)$ (known as input) and $u_{iz}(L) = 0$. More details about this model are given in [6].

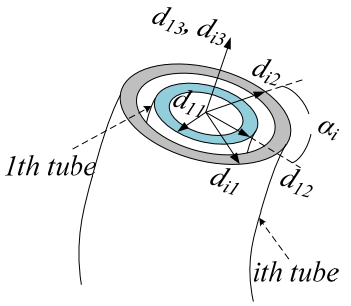

Figure 2. Body frames of tube *i* and the *1st*.

C. Fast Torsionally Compliant Model

As discussed above, the torsionally compliant model is a set of differential equations with two-point boundary conditions. These equations consume a large amount of computational time but only result in a curvature function with respect to the arc length. This function then requires two integrations to calculate the position and orientation of the robot [6]. In our new model, we reformulate the torsionally compliant model with global variables. So the two step calculations can be compressed into one. The bridge between local and global variables lies in (2) and (3) where the rotation matrix $R(s)$ can be parameterized with Euler angles:

$$R(s) = R(\theta_1(s))R(\theta_2(s))R(\theta_3(s)) \tag{8}$$

Substituting (8) into (2), the expressions of curvatures using Euler angles are obtained [12] (arc length s will be omitted for compact expressions):

$$\begin{aligned} u_x &= \dot{\theta}_1 \cos\theta_2 \cos\theta_3 + \dot{\theta}_2 \sin\theta_3 \\ u_y &= \dot{\theta}_2 \cos\theta_3 - \dot{\theta}_1 \cos\theta_2 \sin\theta_3 \\ u_z &= \dot{\theta}_3 + \dot{\theta}_1 \sin\theta_2 \end{aligned} \tag{9}$$

In the same manner, the relationship between positions and Euler angles is obtained by solving (3) [12]:

$$\begin{aligned} \dot{x} &= \sin\theta_2 \\ \dot{y} &= -\sin\theta_1 \cos\theta_2 \\ \dot{z} &= \cos\theta_1 \cos\theta_2 \end{aligned} \tag{10}$$

in which x, y, z are position coordinates in world frame. Applying (9) on the torsionally compliant model (5), (6) and (7), we get:

$$\dot{\theta}_1 = \frac{u_{ix}\cos\theta_{i3} - u_{iy}\sin\theta_{i3}}{\cos\theta_2}$$

$$\dot{\theta}_2 = u_{ix}\sin\theta_{i3} + u_{iy}\cos\theta_{i3} \tag{11}$$

$$\dot{\theta}_{i3} = u_{iz} - \dot{\theta}_1 \sin\theta_2$$

$$\alpha_i(s) = \theta_{i3}(s) - \theta_{13}(s) \tag{12}$$

$$\begin{bmatrix} u_{ix} \\ u_{iy} \end{bmatrix} = \left(\sum_{j=1}^{n} K_j \right)^{-1} R_z^T(\theta_{i3} - \theta_{13}) \left(\sum_{j=1}^{n} R_z^T(\theta_{j3} - \theta_{13}) K_j \begin{bmatrix} \hat{u}_{jx} \\ \hat{u}_{jy} \end{bmatrix} \right) \tag{13}$$

where θ_{i3} represents the 3rd Euler angle of tube *i*. As shown in Fig. 2, all tubes share the same θ_1 and θ_2.

Equations (6), (10), (11) and (13) form the new torsionally compliant model with Euler angles. Solving these equations directly gives the information of position and orientation. One drawback of this model is that (11) has a singular point at $\theta_2 = 90°$, but in most applications that angle is not close to $90°$. The initial conditions of these equations are directly known from inputs, except one of which need to be calculated:

$$u_{iz}(0) = \frac{Torque}{k_{iz}} \tag{14}$$

in which *Torque* is the value measured from Force/Torque sensor attached at the proximal end of the tubes.

This model can be simplified (by piecewise linearization) to a set of linear differential equations. Considering the new kinematic model as a vector function ($\overline{f}(u_{iz} \quad \theta_1 \quad \theta_2 \quad \theta_{i3} \quad x \quad y \quad z)$), and applying the Taylor series expansion, we get:

$$\begin{bmatrix} \dot{u}_{iz} & \dot{\theta}_1 & \dot{\theta}_2 & \dot{\theta}_{i3} & \dot{x} & \dot{y} & \dot{z} \end{bmatrix}^T = \begin{bmatrix} a_1 & a_2 & a_3 & a_4 & a_5 & a_6 & a_7 \\ b_1 & b_2 & b_3 & b_4 & b_5 & b_6 & b_7 \end{bmatrix}^T \begin{bmatrix} 1 \\ s \end{bmatrix} \tag{15}$$

By solving (15), a closed-form kinematic model is obtained for each linear model:

$$\begin{bmatrix} u_{iz} & \theta_1 & \theta_2 & \theta_{i3} & x & y & z \end{bmatrix} = \overline{g}(s) + \overline{C} \tag{16}$$

where all entries in $\overline{g}(s)$ are second-order polynomials, and the vector $\overline{C}$ denotes the initial conditions. The accuracy of (16) is very good when *s* is small. So in the implementation of full model, it is necessary to divide the whole robot into segments and use the linear model consecutively.

III. Experiments

For verifying the fast kinematic model, experiments were performed on four pairs of elastic tubes. The material chosen for these tubes was Nitinol, because of its shape setting property and linear elastic behavior. The specifications of all tube pairs are listed in Table I. The setup for the experiments is shown in Fig. 3. The outer tube was fixed, and the inner tube was rotated with the motorized stage. The force/torque sensor was installed at the base of the outer tube. An EM (electromagnetic) tracker was installed on the tip of the tube pair using a plastic adaptor. The position of the robot's tip can be obtained from the EM tracking system. The effect of gravity as a result of the EM tracker and adaptor was negligible. Since the field generator has the strongest magnetic field in the middle front, the tip of the robot was positioned there to obtain the best accuracy. While this tracking system is accurate to within 1mm, a larger error may occur depending on the accuracy of the method of registration between the tracker and the robot.

It should be noted that the angles read from the rotary stage are not the inputs of our model. Actually, because of

TABLE I
PARAMETERS OF FOUR TUBE PAIRS

Tube pair	**1**	**2**	**3**	**4**
l(mm) [a] **outer/inner**	0/52.8	0/63.5	0/63.5	0/56.4
L(mm) [a] **outer/inner**	152.6/152.6	157/157	157/157	157/157
r(mm) [a] **outer/inner**	250/250	150/150	150/150	150/150
Stiffness ratio outer/inner	1/1.79	1/1.30	1/0.76	1/1.79

a. The lengths of straight and curved sections of tubes are represented by *l* and *L*, respectively. The radius of curvature is denoted as *r*.

the torsional effect in the straight part of the tube pair, the inputs need to be calculated as:

$$\theta_{13}(0) = 0 + \frac{Torque}{k_{1z}} l_1 \,,\; \theta_{23}(0) = Angle - \frac{Torque}{k_{2z}} l_2 \qquad (17)$$

where *Angle* is the angular position of the rotary stage. The positions measured in the experiments are relative to the starting point of the curved section of the robot. In the experiments, the torque at the proximal end was measured and used as the initial condition for the fast kinematic model. For these tube pairs, the final position was obtained by applying the linear model on 10 mm length segments consecutively (16 segments in total for a robot of 157 mm length). The results showed that the loss of accuracy due to linearization is around 0.1 mm. The difference between the positions predicted by the fast kinematic model and the corresponding values measured during the experiment denotes the errors resulting from the model. As shown in Table II, these errors are similar to those in [8]. Because the main parameters of the tube pair used here (curvature, length of tube, and stiffness ratio) are almost the same as those in [8], we can conclude that our model possesses good accuracy. In terms of the computational time, the fast torsionally compliant kinematic model only takes 0.2~0.3 ms to solve. For a 3-tube robot, this time will not exceed 1ms. All the programs were run in Matlab R2010a, under Windows XP, in a computer with an Intel Xeon 3.2 GHz processor. In a future implementation, we expect to obtain further improvement in computational time by coding the algorithm in C++.

IV. Conclusion

Concentric-tube robots are a new technology which has excellent potential for applications in minimally invasive surgery and therapy. Several different kinematic models for this robot have been developed. However, most models suffer from the problem of computational cost in evaluation of the models. A new approach has been developed that significantly reduces the computation cost by reformulating the model in global variables, avoiding two-point boundary problems and by linearization. Experiments for several tube pairs having comparable parameters (lengths of the tubes, stiffness ratio, etc) as those reported in the literature took a lot less computation time while giving similar accuracy. Our ongoing work is aimed at extending the approach for the Jacobian and also designing a model-based robust control scheme that will allow us to address to some extent the effect of uncertainty due to dynamic changes, sensor noise, etc.

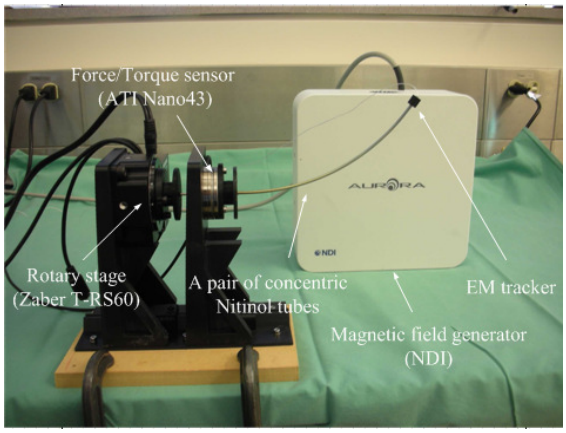

Figure 3. Experimental setup for evaluating kinematic model.

TABLE II
Position Errors Of Tube Pairs

Rotary Stage Angle (deg)		**0**	**60**	**120**	**180**	**240**	**300**	**Average**	**Max**
Position Errors (mm)	**Pair 1**	0.7	1.8	1.0	1.7	1.8	1.7	1.5 (1.0%) [a]	1.9
	Pair 2	1.3	0.7	3.1	8.1	3.1	1.8	3.0 (1.9%)	8.1
	Pair 3	1.4	1.8	1.9	10.0	4.0	2.6	3.5 (2.2%)	10.0
	Pair 4	1.2	4.9	2.8	9.0	5.7	4.4	4.7 (3.0%)	9.0

a. Values in brackets are normalized errors (the tip errors divide by the length of robot).

Acknowledgment

The authors would like to thank Johnson Matthey Inc. for providing the Nitinol tubes used in the experimental work described in this paper. The assistance of the CSTAR research team, in particular doctoral student, Mr. Ali Asadian, is gratefully acknowledged.

References

[1] J. Furusho, T. Katsuragi, T. Kikuchi, T. Suzuki, H. Tanaka, Y. Chiba, and H. Horio, "Curved multi-tube systems for fetal blood sampling and treatments of organs like brain and breast," *J. Comput. Assist. Radiol. Surg.*, vol. 1, pp. 223–226, 2006.

[2] P. Sears and P. E. Dupont, "A steerable needle technology using curved concentric tubes," *IEEE/RSJ Int. Conf. on Intelligent Robots and Systems*, pp. 2850–2856, 2006.

[3] P. Sears and P. E. Dupont, "Inverse kinematics of concentric tube steerable needles," *IEEE Int. Conf. on Robotics and Automation*, pp. 1887–1892, 2007.

[4] R. J. Webster III, J. M. Romano, and N. J. Cowan, "Mechanics of precurved-tube continuum robots," *IEEE Trans. Robot.*, vol. 25, no. 1, pp. 67–78, 2009.

[5] R. J. Webster III, J. P. Swensen, J. M. Romano, and N. J. Cowan, "Closed-form differential kinematics for concentric-tube continuum robots with application to visual servoing," *Int. Symposium on Experimental Robotics*, 2008.

[6] P. Dupont, J. Lock, B. Itkowitz, and E. Butler, "Design and control of concentric-tube robots," *IEEE Trans. Robot.*, vol. 26, no. 2, pp. 209–225, 2010.

[7] D. C. Rucker and R. J. Webster III, "Mechanics-based modeling of bending and torsion in active cannulas," *IEEE RAS/EMBS Int. Conf. on Biomedical Robotics and Biomechatronics*, pp.704–709, 2008.

[8] J. Lock and P. E. Dupont, "Friction modeling in concentric tube robots," *IEEE Int. Conf. on Robotics and Automation,* pp. 1139–1146, 2011.

[9] D. C. Rucker, B. A. Jones, and R. J. Webster III, "A geometrically exact model for externally loaded concentric-tube continuum robots," *IEEE Trans. Robot.*, vol. 26, no. 5, pp. 769–780, 2010.

[10] P. Dupont, J. Lock, and B. Itkowitz, "Real-time position control of concentric tube robots," *Conf Proc IEEE Int. Conf. on Robotics and Automation*, pp. 562–568, 2010.

[11] D. C. Rucker, and R. J. Webster III, "Computing jacobians and compliance matrices for externally loaded continuum robots," *IEEE Int. Conf. on Robotics and Automation*, pp. 945–950, 2011.

[12] I. G. Tadjbakhsh and D. C. Lagoudas, "Variational theory of motion of curved, twisted and extensible elastic rods," *Int. J. Eng. Sci.*, vol. 32, no. 4, pp. 569–577, 1994.

[13] S. S. Antman, *Nonlinear problems of elasticity*, Springer Verlag, New York, 1995.